

# Proton irradiation-induced reliability degradation of SiC power MOSFET

K. Niskanen, *Member, IEEE*, H. Kettunen, *Member, IEEE*, D. Söderström, *Student Member, IEEE*, M. Rossi, *Member, IEEE*, J. Jaatinen, *Member, IEEE* and A. Javanainen, *Member, IEEE*

**Abstract**—The effect of 53 MeV proton irradiation on the reliability of silicon carbide power MOSFETs was investigated. Post-irradiation gate voltage stress was applied and early failures in time-dependent dielectric breakdown (TDDB) test were observed for irradiated devices. The applied drain voltage during irradiation affects the degradation probability observed by TDDB tests. Proton-induced single event burnouts (SEB) were observed for devices which were biased close to their maximum rated voltage. The secondary particle production as a result of primary proton interaction with the device material was simulated with the Geant4-based toolkit.

**Index Terms**—Power MOSFET, proton irradiation, silicon carbide (SiC), single event burnout (SEB), time-dependent dielectric breakdown (TDDB)

## I. INTRODUCTION

SILICON carbide (SiC) has recently gained interest in power electronics applications due to its superior material properties over silicon. SiC has high critical electric field, high thermal conductivity and high melting point which are favourable properties where high power density is needed [1]. However, it has been found that SiC power devices are sensitive to destructive single event effects due to radiation impact in space and atmospheric environments [2]–[4].

Many of the studies which reported radiation effects on such devices focus on catastrophic effects, such as single event burnout (SEB) and single event gate rupture (SEGR). The degradation of gate oxide and drain leakage in SiC power devices due to heavy ion and neutron impact has been reported in several studies [5]–[11]. The proton induced SEB [12]–[14] and parameter degradation [15], [16] in SiC power devices have been observed but those studies do not take into account the effect of proton irradiation on the long-term reliability of the devices.

During their operation in the space environment, on top of the radiative stress, those devices are exposed to electrical stress, and as for any system, reliable operation of power

electronics devices is needed for full desired lifetime of the system. Therefore, on top of the sensitivity to catastrophic failures, it is important to assess if the operation in radiation environments causes a reduction in long-term reliability of these devices.

Regarding the overall reliability of SiC MOSFETs, the gate oxide degradation remains an issue [17], [18]. Even though the intrinsic reliability of the gate SiO<sub>2</sub> has improved over the years, the material defects as well as the radiation impact have a significant effect on the oxide reliability [4]–[9], [19], [20]. On top of that, it is known that gate reliability of SiC MOSFETs is degraded during switching operation due to the "reach-through phenomenon", where the high electric field caused by the applied drain bias, is relocated closer to the gate oxide layer [21]. Therefore, it is reasonable to assume that the non-destructive radiation interaction can have an impact on the gate oxide integrity during device operation due to the charge generation and transport in the device structure.

The reliability tests for devices that have survived atmospheric neutron irradiation have shown very little effect of radiation on the device degradation [22]–[24]. However, those tests were performed with devices from a different manufacturer than in this study.

In this work, we investigate the effect of 53 MeV proton radiation on SEB sensitivity and on long term reliability of SiC power MOSFETs through accelerated voltage stress experiments.

## II. EXPERIMENTAL DETAILS

### A. Device under test

The device under test (DUT) is a commercial 4H-SiC power MOSFET manufactured by Wolfspeed (part number C3M0350120D). A total of 50 samples were tested of which 40 were irradiated and 10 devices was used per bias condition. All the devices were electrically characterized before and after irradiation.

### B. Radiation experiment

Proton irradiations were performed at RADEF (RADIATION Effects Facility) at the University of Jyväskylä, Finland. The 53 MeV proton beam was obtained from the K130 cyclotron in the Accelerator Laboratory at the University of Jyväskylä. During irradiations, the devices were connected in parallel. The gate-to-source voltage  $V_{GS}$  was set to 0 V and drain-to-source voltages  $V_{DS}$  of 400 V, 600 V, 800 V and 1000 V were applied on the devices and the total current was monitored

Manuscript received October 14, 2022; revised December 20, 2022 and January 10, 2023.

K. Niskanen, H. Kettunen, M. Rossi, J. Jaatinen, D. Söderström and A. Javanainen are with Accelerator Laboratory, Department of Physics, University of Jyväskylä, P.O. Box 35, FI-40014 University of Jyväskylä, Finland (e-mail: kimmo.h.niskanen@jyu.fi).

A. Javanainen is also with Electrical and Computer Engineering Department, Vanderbilt University, Nashville, TN 37235, USA

This work has been supported by the European Space Agency (ESA/ESTEC Contract No. 124504/18/NL/KML/zk).

We acknowledge grants of computer capacity from the Finnish Grid and Cloud Infrastructure (persistent identifier urn:nbn:fi:research-infras-2016072533).

with a Keithley 2470 source measure unit (SMU). DUTs were irradiated with proton beam flux of  $10^8 \text{ cm}^{-2} \text{ s}^{-1}$  up to  $10^{11} \text{ cm}^{-2}$  total fluence. The flux was considered to be constant within 10% uncertainty among the runs and over the DUT area.

### C. Accelerated wear-out experiment

In order to investigate if the proton radiation has an impact on the long term reliability of SiC power MOSFET, an accelerated wear-out procedure was applied on the devices which did not exhibit SEB after irradiation. Irradiated devices, as well as one set of pristine devices, were exposed to a constant voltage stress (CVS) at the gate terminal, while the drain and the source terminals were grounded. Similar accelerated wear-out procedures have been applied in [20], [25].

Based on the Fowler-Nordheim (FN) curves measured for three randomly picked devices, a  $V_{GS}$  of 36 V was chosen as the stress voltage. Such a  $V_{GS}$  value results in initial  $I_{GS}$  of approximately  $10 \mu\text{A}$ . The chosen  $V_{GS}$  value is well below the instantaneous breakdown voltage of the gate oxide, but at the same time, above the normal operating voltage in order to accelerate the wear-out effect. The CVS was applied and the  $I_{GS}$  was monitored until an abrupt increase in  $I_{GS}$  was observed. The time at which that increase occurred, was then defined as the time-to-breakdown ( $T_{BD}$ ).

While assuming 50 nm oxide thickness, a resulting  $E_{ox}$  of  $7.2 \text{ MV cm}^{-1}$  was applied across the oxide layer. By choosing such a value for  $E_{ox}$ , we are able to collect  $T_{BD}$  data in an accelerated manner while staying below the critical  $E_{ox}$  ( $> 10 \text{ MV cm}^{-1}$ ) [26] in order to avoid immediate device failure during CVS. Also, the electric field is below the value where the electric field acceleration factor for higher fields plays a role, when performing the reliability analysis based on the time-dependent dielectric breakdown (TDDB) results [20], [25].

## III. RESULTS AND DISCUSSION

### A. Proton-induced SEB

The heavy ion irradiation experiments on 1200 V SiC power devices have shown that the SEB threshold dependence on the linear energy transfer (LET) follows the so-called "hockey stick" trend [3]. The SEB threshold saturates approximately to 500 V for  $\text{LET} > 10 \text{ MeV cm}^2 \text{ mg}^{-1}$ . Moreover, the SEB threshold for LET of  $1 \text{ MeV cm}^2 \text{ mg}^{-1}$  is  $\sim 1100 \text{ V}$ , which is close to the maximum rated voltage of the devices. However, the LET value of the 53 MeV protons used in this study is only  $0.01 \text{ MeV cm}^2 \text{ mg}^{-1}$  and therefore, it is not expected to be sufficient in order to induce SEB due to direct ionization. However, the secondary particles produced during the interaction of primary protons with the target material nuclei can have a higher LET and could therefore cause SEB. This will be discussed further in III-D.

Since the proton interaction with the target nuclei is a stochastic process, to determine the proton induced SEB sensitivity, we applied the two-parameter Weibull cumulative distribution function (CDF)

$$F(x) = 1 - e^{-\left(\frac{x}{\eta}\right)^\beta}, \quad (1)$$

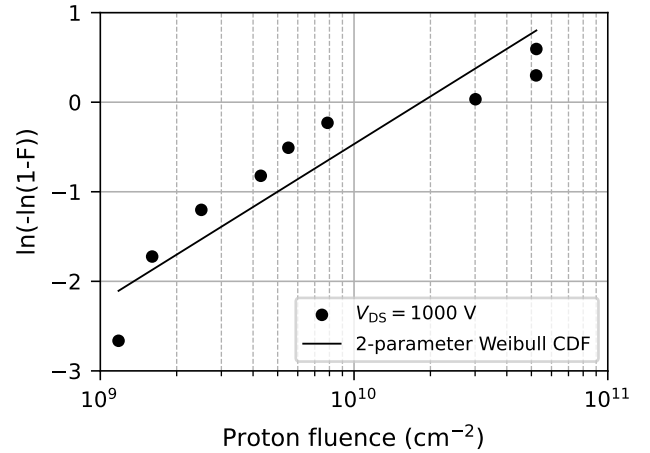


Fig. 1. Weibull plot of proton-induced SEB failures for devices irradiated at  $V_{DS} = 1000 \text{ V}$ . 9 of the 10 irradiated devices exhibited SEB during irradiation test. The line represents the fitting of 2-parameter Weibull CDF in the SEB data. The  $r^2$ -value for the fit is 0.87.

where  $\beta$  is the shape parameter and  $\eta$  is the scale parameter of the Weibull distribution. The scale parameter  $\eta$  represents the fluence when 63% of the test population has failed [27]. The Weibull distribution has been used previously in analysis of neutron-induced SEB [4], [22], [28].

In order to compare the empirical data with the distribution function, a common way to obtain the  $y$ -coordinate for each failure is to apply the Benard approximation (2):

$$F = \frac{i - 0.3}{N + 0.4}, \quad (2)$$

where  $i$  is the running number of the failure (first, second etc.) and  $N$  is the sample size. Then, rewriting (1) gives:

$$\ln(-\ln(1 - F)) = \beta \ln(x) - \beta \ln(\eta). \quad (3)$$

For each device failure,  $\ln(-\ln(1 - F))$  was then plotted as a function of proton fluence until corresponding failure (Fig. 1). Equation (1) was then fitted to the failure data. Based on the extracted Weibull parameters  $\beta$  and  $\eta$ , we calculated the mean fluence to failure (MFTF):

$$\text{MFTF} = \eta \times \Gamma\left(1 + \frac{1}{\beta}\right), \quad (4)$$

where  $\Gamma$  is the gamma function. For the devices which were irradiated at  $V_{DS} = 1000 \text{ V}$ , we observe 9 failures over the total of 10 irradiated devices. For the other irradiation voltages ( $V_{DS} = 400 \text{ V}$ ,  $600 \text{ V}$  and  $800 \text{ V}$ ), no failures were observed during irradiations until the goal fluence was reached. The extracted  $\eta$  and  $\beta$  values for the SEB distribution are  $(2.1 \pm 0.8) \times 10^{10} \text{ cm}^{-2}$  and  $0.73 \pm 0.20$  respectively at the 95% confidence interval. Based on those values, the calculated MFTF is  $2.6 \times 10^{10} \text{ cm}^{-2}$  for the  $V_{DS} = 1000 \text{ V}$  irradiation voltage configuration.

The shape parameter  $\beta$  is an indicator of failure rate behavior. If  $\beta < 1$ , the population will show a decreasing failure rate with time, which is representative of early life

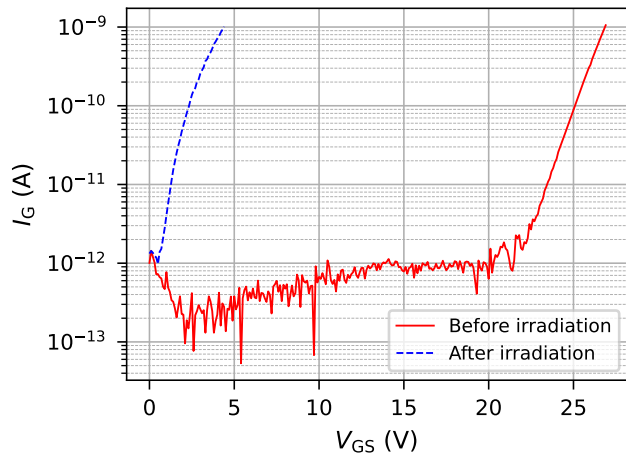


Fig. 2. Gate current for the one device which did not exhibit failure after the SEB test. The device was irradiated at  $V_{DS} = 1000$  V. High gate leakage current at  $V_{GS} < 5$  V indicates device failure.

failures. Moreover,  $\beta = 1$  is representative of random failures which is related to a constant failure rate over time. For the proton-induced SEB failure distribution in this study, the  $\beta$  value is close to one, indicating random failure over time, which has also been observed with neutron-induced SEB in SiC power MOSFETs [4], [28].

Post-irradiation characterization reveals gate oxide degradation for the survived device from the SEB test. The gate current during gate voltage sweep in Fig. 2 shows high leakage already at  $V_{GS} < 5$  V. Such strong degradation means that even if the device did not undergo SEB during irradiation, it is still considered as failed. For the rest of the devices which were exposed to irradiation at 1000 V and suffered SEB, the gate was found to be totally failed. Whereas the  $I_{GS}V_{GS}$  characteristics of the survived device resembles the  $I_{GS}V_{GS}$  characteristics of a fresh device but with strong degradation as shown in Fig. 2, the gate current for SEB failed devices reached 1 A compliance of the SMU as soon as the gate voltage sweep was started.

### B. TDDB of survived devices

As mentioned in III-A, not all the devices exhibit SEB during irradiations. In order to reveal possible irradiation induced gate oxide weakening, in addition to post-irradiation IV-characterizations, a CVS method described in II-C was applied for both non-irradiated and irradiated devices. Time-to-breakdown  $T_{BD}$  was recorded for each device during the CVS test.  $T_{BD}$  was defined as the time when an abrupt increase in  $I_{GS}$  was observed and the  $I_{GS}$  exceeded 1 mA. Fig. 3 shows the gate current evolution during CVS for devices which were irradiated at  $V_{DS} = 600$  V. For most of the devices, the gate current increases during the stress and after that, starts to decrease before the breakdown. However, for some of the devices the failure occurs already during the increasing current phase and on top of that, much earlier than for the rest of the devices in the set. Such differences in the breakdown

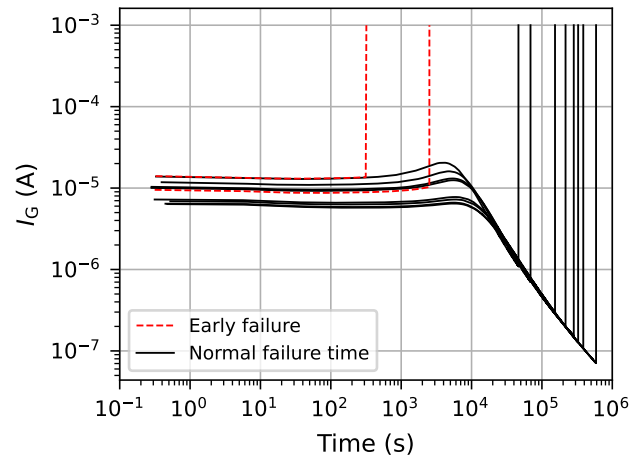


Fig. 3. Gate current in CVS ( $V_{GS} = 36$  V) for proton-irradiated parts. An abrupt increase in the gate current indicates the oxide breakdown. Two parts of the batch exhibit early failure. Devices were irradiated at  $V_{DS} = 600$  V.

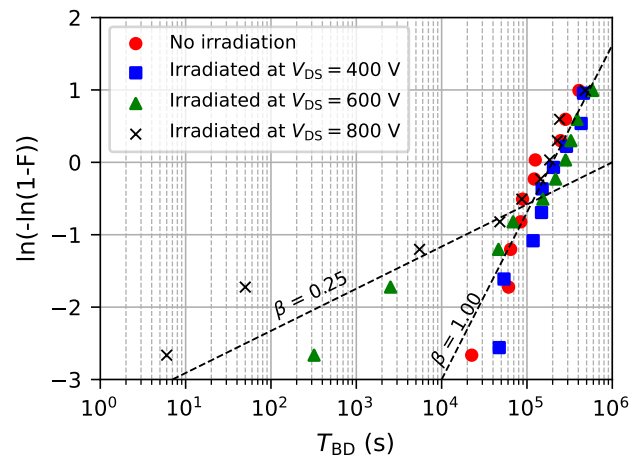


Fig. 4. Weibull plot of  $T_{BD}$  for fresh and irradiated devices. The extrinsic tail of early failures can be seen for devices irradiated at  $V_{DS} = 600$  V and 800 V. The dashed lines are given as a guide to the eye to emphasize the two different breakdown mechanisms. In general,  $\beta < 1$  indicates early failures.

behaviour between the devices will be discussed further in this section.

The TDDB of the gate oxide, when the applied oxide electric field ( $E_{ox}$ ) is below the critical oxide electric field, is said to occur due to the trap generation by charge injection in the oxide layer. After reaching the critical trap density, a conducting path through the gate oxide is formed which results in oxide breakdown [29]. Therefore, comparing the  $T_{BD}$  distributions of fresh and irradiated devices can give some information about the impact of radiation on the long term reliability of the devices.

Fig. 4 shows the  $T_{BD}$  distribution for irradiated and fresh devices. It seems that the breakdown time of the irradiated devices exhibits two distinguishable behaviours. Five irradiated devices undergo early breakdown whereas the rest of the

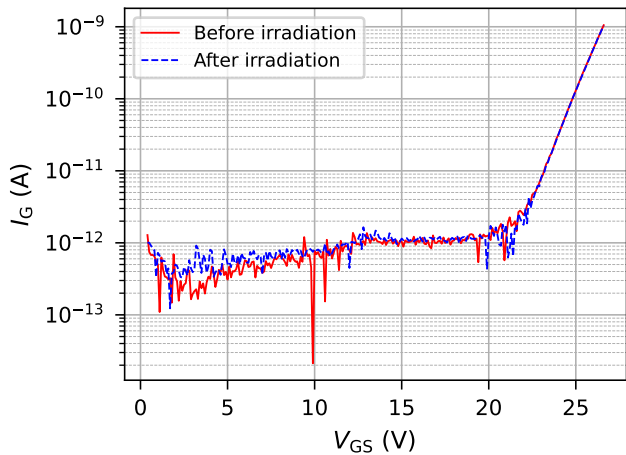


Fig. 5. The Fowler-Nordheim curves for a device before and after proton exposure.  $V_{DS} = 800$  V during irradiation. This device suffered early failure at  $T_{BD} = 50$  s. In order to minimize the damage induced by the charge injection during the characterization, the  $V_{GS}$  sweep was stopped when  $I_{GS}$  reached 1 nA.

batch seem to follow the the same wear-out failure behaviour as the fresh devices. Such an extrinsic tail in failure behaviour in Fig. 4 could be related to proton-induced defects and the current transport through the gate oxide layer by the trap-assisted tunneling (TAT) process [19]. Either the secondary particles produced by the primary proton beam induce damage through the ionization track within the oxide layer or through the current transient occurring in the epitaxial layer and subsequent electric field transient in the gate oxide. Nonetheless, it seems that the proton irradiation increases the defect density in the oxide layer which results in increase of early failures in the TDDB test. Moreover, since the proton interaction with the target material nuclei is a stochastic process, it seems that some of the parts within the irradiated batch remain unaffected by the proton impact while some exhibit strong degradation revealed by the voltage stress. This is a strong indication that the direct ionization alone induced by protons at this fluence does not have a significant contribution to the oxide degradation.

Fig. 5 and Fig. 6 show representative pre- and postirradiation characteristics for one device, which suffered an early failure during CVS ( $T_{BD} = 50$  s). No increased leakage currents were observed after the proton irradiation. Even the devices which suffered early failures during CVS, show no degradation in their IV-characteristics. Therefore, unlike for the parts under heavy ion irradiation exposure, it is not possible to predict the proton-induced oxide weakening from the postirradiation characteristics. Here, the proton-induced defects are of random nature and spatially localized. Therefore, we do not observe significant leakage current increases or threshold voltage shift after irradiation. However, even very localized damage in the gate oxide layer can act as a precursor for an early failure.

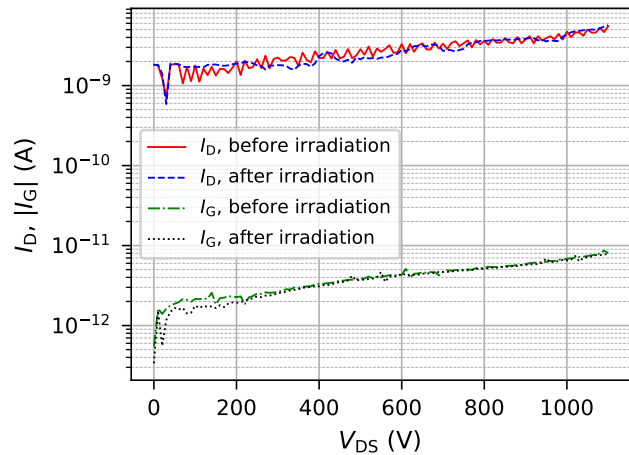


Fig. 6. Pre- and postirradiation  $I_D V_{DS}$  and  $I_G V_{DS}$  curves for a device which exhibited early failure ( $T_{BD} = 50$  s) during CVS. Such characteristics do not predict early breakdown.

### C. The effect of irradiation bias on stress-induced failure

As mentioned earlier, the SEB sensitivity of SiC power devices is dependent on the particle LET and applied drain voltage during irradiation. Also, the bias voltage and LET dependence on the heavy ion induced charge collection and leakage current have been observed [10], [11]. As we observed in III-A, the survived device from the SEB experiment exhibited a strong gate oxide degradation. Therefore, we look more closely at the irradiation bias dependence on the TDDB characteristics in order to see if similar to SEB and to single event leakage current (SEL), but weaker irradiation-induced damage can be observed for the lower irradiation bias configurations. Fig. 4 shows the TDDB distributions for devices irradiated at different drain bias voltages. Higher drain voltage during irradiation results in higher number of early failures which can originate from higher radiation-induced degradation of the device. The closer the applied irradiation voltage is to the SEB threshold voltage, the higher the probability of observing early failures during TDDB test. This trend suggests that the irradiation-induced gate oxide degradation is related to the charge generation and transport in the drift layer of the MOSFET during the ion impact.

When an ionizing particle hits the device epitaxial layer, the generated charge will be collected. During the charge transport, the holes are accumulated below the gate oxide layer which results in an elevated electric field in the oxide layer. This phenomenon is enhanced with increasing drain bias voltage.

### D. Simulation of secondary particles

The mechanism for irradiation-induced degradation for SiC power devices is said to be related to the peak power  $P_{peak}$  dissipated at the ion strike location [10], [11]. The peak power is estimated to be proportional to the product of deposited energy of secondary particle ( $E_{dep}$ ) and square of applied drain voltage during irradiation:

$$P_{\text{peak}} \propto E_{\text{dep}} \times V_{\text{DS}}^2. \quad (5)$$

In order to understand the secondary particle spectrum and deposited energy induced by the proton impact, we performed Monte Carlo simulations by using the Geant4 based simulation toolkit G4SEE [30]. In the simulation, the target dimensions were  $1.8 \text{ mm} \times 2.8 \text{ mm}$  with a  $300 \mu\text{m}$  thickness of the SiC substrate. In the G4SEE simulation, a  $10 \mu\text{m}$  thick SiC layer was defined as the sensitive volume (SV) at the top of the SiC layer. This thickness corresponds to the thickness of the epitaxial layer. In addition,  $2 \text{ mm}$  of plastic and  $15 \mu\text{m}$  of Al were added on the top of the sensitive volume in order to represent the packaging and the back end of line (BEOL) layer (Fig. 7). The densities of the materials used in the simulation are  $3.21 \text{ g cm}^{-3}$ ,  $2.7 \text{ g cm}^{-3}$  and  $1.2 \text{ g cm}^{-3}$  for SiC, Al and plastic respectively. Based on the TRIM [31] calculations, the range of the  $53 \text{ MeV}$  protons in SiC is  $9.37 \text{ mm}$ . However, the device has other materials than SiC but those materials are expected to be similar or lower in density and since the thickness of the device is approximately  $5 \text{ mm}$ , the range of the protons is expected to exceed the device thickness. From the simulated particle spectrum in the SV, the secondary particles with impact angles within  $30^\circ$  of normal incidence and with ranges over  $5 \mu\text{m}$  were included in the analysis. In addition, only the particles which were produced at maximum  $1 \mu\text{m}$  below the gate oxide layer were included. By setting such constraints, we are more likely focusing only on the relevant secondary particles regarding the energy deposition and distance traveled in the epitaxial layer which might contribute to the gate oxide degradation of the device.

Since the experimental data suggests that the gate oxide degradation is drain voltage dependent, we assume here that the gate oxide degradation is originating from the similar charge generation and transport mechanism as the more severe SEB and SELC. Therefore, we apply (5) to the energy deposition spectrum from the G4SEE simulations. Fig. 8 shows the complementary cumulative distribution functions (CCDF) for peak power of secondary events induced by the primary proton beam. The critical power for degradation ( $P_{\text{crit}}$ ) has been defined based on the experimentally observed absence of early failures when devices were biased at  $V_{\text{DS}} = 400 \text{ V}$ . For that irradiation bias voltage configuration, the power dissipated at the charge generation location does not exceed  $P_{\text{crit}}$  whereas when increasing the drain voltage during irradiation, the probability of an event whose  $P_{\text{peak}}$  exceeds  $P_{\text{crit}}$ , increases.

From the deposited energy obtained in the G4SEE simulations, we calculated a quasi LET value for each secondary particle by dividing the  $E_{\text{dep}}$  by the range in SV. Since the majority of the heavy secondary particles in SV stop or are very close to being at the end of their range, their LET value varies significantly along the track. Therefore, this value represents an average value of LET along the track and can be somewhat comparable to the LET values, which have been reported in heavy-ion tests.

When looking at the nature and the quasi LET of the secondary particles in Fig. 9, we can see that the most

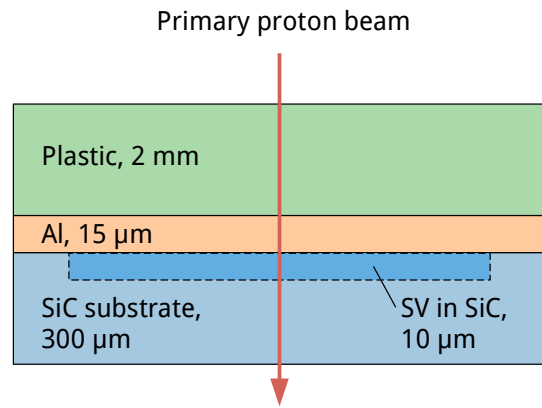


Fig. 7. The geometry of the simulation model implemented in G4SEE. The SV where the secondary particle spectrum is observed is drawn with dashed line. The thicknesses of the layers are not to scale.

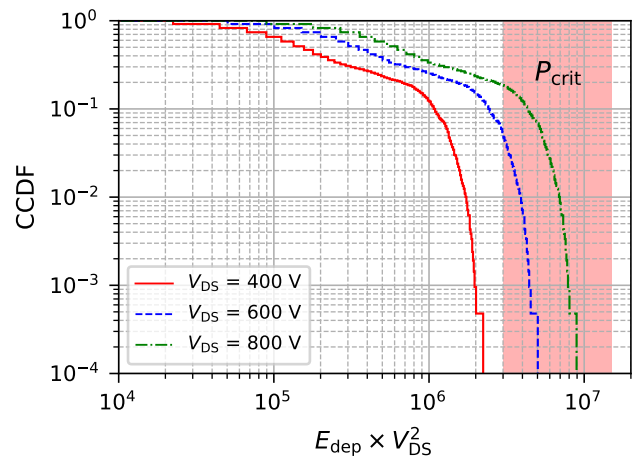


Fig. 8. Peak power in the SV for different drain bias configurations calculated after (5). The red shaded region represents the critical power dissipation needed for permanent damage in the device structure.

abundant are the lighter particles with low quasi LET, below  $2 \text{ MeV cm}^2 \text{ mg}^{-1}$ . Those particles are expected to have less contribution to the degradation and SEB. However, there is still a probability of generating heavier particles with higher quasi LET, even up to  $8 \text{ MeV cm}^2 \text{ mg}^{-1}$ . This value is consistent with the data presented in [3], where the SEB threshold increases significantly below the LET of  $10 \text{ MeV cm}^2 \text{ mg}^{-1}$ . However, even below that LET, it is still possible to observe SEBs, when the devices are biased close to their maximum operating voltage limit, as was also observed in this study at  $V_{\text{DS}} = 1000 \text{ V}$ . Moreover, since the LET of the secondary particles is high enough to induce SEB, it should be sufficient to induce damage in the device when the bias applied to the device is further below the maximum operating limit.

#### IV. CONCLUSION

The sensitivity of SiC power MOSFETs to SEB and latent damage under proton irradiation has been investigated. A long term reliability degradation of the SiC power MOSFET due to proton irradiation was observed.

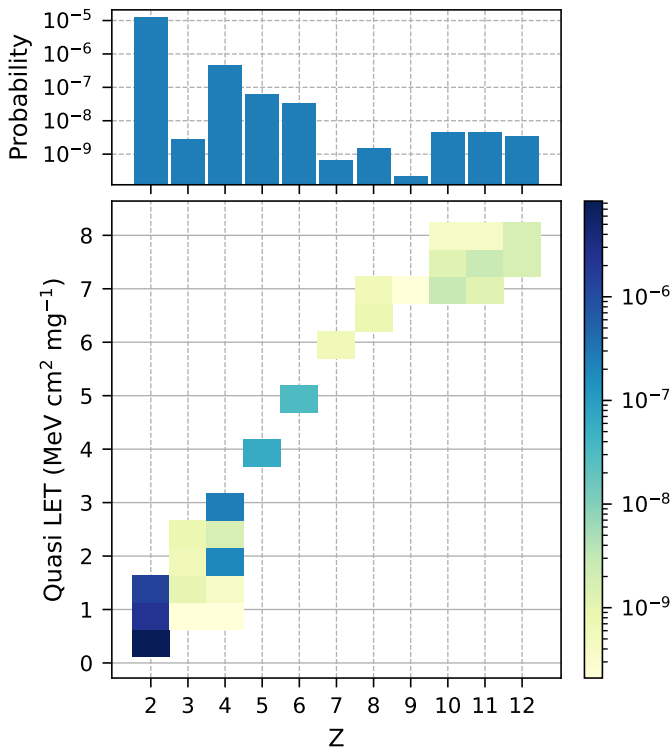


Fig. 9. A histogram of probabilities of particle types generated by the primary proton beam (top) and a 2D histogram (bottom) of the quasi LET and atomic number  $Z$  of secondary particles from primary proton beam interactions in the SV. The color bar represents the particle occurrence probability for a specific quasi LET interval and  $Z$ . A total of  $5 \times 10^6$  primary particles were used in the simulation.

None of the non-failed devices during irradiations exhibit increased leakage current during post-irradiation characterizations in the rated safe voltage region. However, as we have seen here, even if no failure is observed during the post-irradiation voltage sweeps, it does not imply that the gate oxide is not weakened due to the non-destructive proton impact. This was demonstrated through the accelerated gate voltage stress test, which shows early failures for devices irradiated already at 50% of their maximum rated drain voltage.

The irradiation drain bias voltage seems to have an impact on the post-irradiation gate failure behavior observed during the CVS test. Such result suggests that the gate oxide degradation is related to the charge generation and transport in the drift layer of the MOSFET due to the secondary ion impact.

The deposited energy spectrum by secondary particles was simulated with the G4SEE toolkit showing that the heavier secondary particles produced by the primary proton beam can have sufficient energy in order to induce damage along their track and therefore, contribute to the weakening of the gate oxide and early failures in the TDDB test.

#### REFERENCES

[1] J. Millan, P. Godignon, X. Perpina, A. Perez-Tomas, and J. Rebollo, "A survey of wide bandgap power semiconductor devices," *IEEE Trans. Power Electron.*, vol. 29, no. 5, pp. 2155–2163, May 2014.

[2] J. M. Lauenstein, M. C. Casey, R. L. Ladbury, H. S. Kim, A. M. Phan, and A. D. Topper, "Space Radiation Effects on SiC Power Device Reliability," in *Proc. IEEE Int. Rel. Phys. Symp. (IRPS)*, Monterey, CA, USA, Mar. 2021, pp. 498–505.

[3] A. F. Witulski, D. R. Ball, K. F. Galloway, A. Javanainen, J. M. Lauenstein, A. L. Sternberg, and R. D. Schrimpf, "Single-Event Burnout Mechanisms in SiC Power MOSFETs," *IEEE Trans. Nucl. Sci.*, vol. 65, no. 8, pp. 1951–1955, Aug. 2018.

[4] K. Niskanen, R. Coq Germanicus, A. Michez, F. Wrobel, J. Boch, F. Saigne, and A. D. Touboul, "Neutron-Induced Failure Dependence on Reverse Gate Voltage for SiC Power MOSFETs in Atmospheric Environment," *IEEE Trans. Nucl. Sci.*, vol. 68, no. 8, pp. 1623–1632, Aug. 2021.

[5] M. Deki, T. Makino, N. Iwamoto, S. Onoda, K. Kojima, T. Tomita, and T. Ohshima, "Linear energy transfer dependence of single event gate rupture in SiC MOS capacitors," *Nucl. Instrum. Methods Phys. Res. Sect. B, Beam Interact. Mater. At.*, vol. 319, pp. 75–78, Jan. 2014.

[6] C. Abbate, G. Busatto, D. Tedesco, A. Sanseverino, F. Velardi, and J. Wyss, "Gate damages induced in SiC power MOSFETs during heavy-ion irradiation-Part I," *IEEE Trans. Electron Devices*, vol. 66, no. 10, pp. 4235–4242, Oct. 2019.

[7] M. Deki, T. Makino, K. Kojima, T. Tomita, and T. Ohshima, "Instability of critical electric field in gate oxide film of heavy ion irradiated SiC MOSFETs," *Mater. Sci. Forum*, vol. 821–823, pp. 673–676, Jun. 2015.

[8] C. Martinella, R. Stark, T. Ziemann, R. G. Alia, Y. Kadi, U. Grossner, and A. Javanainen, "Current Transport Mechanism for Heavy-Ion Degraded SiC MOSFETs," *IEEE Trans. Nucl. Sci.*, vol. 66, no. 7, pp. 1702–1709, Jul. 2019.

[9] C. Martinella, T. Ziemann, R. Stark, A. Tsibizov, K. O. Voss, R. G. Alia, Y. Kadi, U. Grossner, and A. Javanainen, "Heavy-Ion Microbeam Studies of Single-Event Leakage Current Mechanism in SiC VD-MOSFETs," *IEEE Trans. Nucl. Sci.*, vol. 67, no. 7, pp. 1381–1389, Jul. 2020.

[10] S. Kuboyama, C. Kamezawa, N. Ikeda, T. Hirao, and H. Ohyama, "Anomalous charge collection in silicon carbide schottky barrier diodes and resulting permanent damage and single-event burnout," *IEEE Trans. Nucl. Sci.*, vol. 53, no. 6, pp. 3343–3348, Dec. 2006.

[11] A. Javanainen, K. F. Galloway, C. Nicklaw, A. L. Bossler, V. Ferlet-Cavrois, J. M. Lauenstein, F. Pintacuda, R. A. Reed, R. D. Schrimpf, R. A. Weller, and A. Virtanen, "Heavy ion induced degradation in SiC Schottky diodes: Bias and energy deposition dependence," *IEEE Trans. Nucl. Sci.*, vol. 64, no. 1, pp. 415–420, Jan. 2017.

[12] E. Mizuta, S. Kuboyama, H. Abe, Y. Iwata, and T. Tamura, "Investigation of single-event damages on silicon carbide (SiC) power MOSFETs," *IEEE Trans. Nucl. Sci.*, vol. 61, no. 4, pp. 1924–1928, Aug. 2014.

[13] H. Zhang, H. Guo, F. Zhang, Z. Lei, X. Pan, Y. Liu, Z. Gu, A. Ju, X. Zhong, and X. Ouyang, "Study on proton-induced single event effect of SiC diode and MOSFET," *Microelectron. Rel.*, vol. 124, Jun. 2021, Art. no. 114329.

[14] S. Kuboyama, C. Kamezawa, Y. Satoh, T. Hirao, and H. Ohyama, "Single-event burnout of silicon carbide schottky barrier diodes caused by high energy protons," *IEEE Trans. Nucl. Sci.*, vol. 54, no. 6, pp. 2379–2383, Dec. 2007.

[15] A. A. Lebedev, V. V. Kozlovski, L. Fursin, A. M. Strel'chuk, M. E. Levinshtein, P. A. Ivanov, and A. Zubov, "Impact of proton irradiation on power 4H-SiC MOSFETs," *Mater. Sci. Forum*, vol. 1004 MSF, pp. 1074–1080, Jul. 2020.

[16] A. A. Lebedev, V. V. Kozlovski, M. E. Levinshtein, P. A. Ivanov, A. M. Strel'chuk, A. V. Zubov, and L. Fursin, "Effect of high energy (15 MeV) proton irradiation on vertical power 4H-SiC MOSFETs," *Semicond. Sci. Technol.*, vol. 34, no. 4, Mar. 2019, Art. no. 045004.

[17] R. Ouaidia, M. Berthou, J. León, X. Perpiñà, S. Oge, P. Brosselard, and C. Joubert, "Gate oxide degradation of SiC MOSFET in switching conditions," *IEEE Electron Device Lett.*, vol. 35, no. 12, pp. 1284–1286, Dec. 2014.

[18] K. P. Cheung, "SiC power MOSFET gate oxide breakdown reliability-Current status," in *Proc. IEEE Int. Rel. Phys. Symp. (IRPS)*, Burlingame, CA, USA, Mar. 2018, pp. 2B.3.1–2B.3.5.

[19] Z. Chbili, A. Matsuda, J. Chbili, J. T. Ryan, J. P. Campbell, M. Lahbabi, D. E. Ioannou, and K. P. Cheung, "Modeling early breakdown failures of gate oxide in SiC power MOSFETs," *IEEE Trans. Electron Devices*, vol. 63, no. 9, pp. 3605–3613, Sep. 2016.

[20] M. Gurfinkel, Y. Shapira, J. C. Horst, J. S. Suehle, J. B. Bernstein, K. S. Matocha, G. Dunne, R. A. Beaupre, Y. Shapira, K. S. Matocha, G. Dunne, and R. A. Beaupre, "Time-Dependent Dielectric Breakdown of 4H-SiC/SiO<sub>2</sub> MOS Capacitors," *IEEE Trans. Device Mater. Rel.*, vol. 8, no. 4, pp. 635–641, Dec. 2008.

- [21] T. T. Nguyen, A. Ahmed, T. V. Thang, and J. H. Park, "Gate oxide reliability issues of SiC MOSFETs under short-circuit operation," *IEEE Trans. Power Electron.*, vol. 30, no. 5, pp. 2445–2455, May 2015.
- [22] F. Principato, G. Allegra, C. Cappello, O. Crepel, N. Nicosia, S. D. Arrigo, V. Cantarella, A. Di Mauro, L. Abbene, M. Mirabello, and F. Pintacuda, "Investigation of the Impact of Neutron Irradiation on SiC Power MOSFETs Lifetime by Reliability Tests," *Sensors*, vol. 21, no. 16, 2021, Art. no. 5627.
- [23] A. Akturk, R. Wilkins, J. McGarrity, and B. Gersey, "Single Event Effects in Si and SiC Power MOSFETs Due to Terrestrial Neutrons," *IEEE Trans. Nucl. Sci.*, vol. 64, no. 1, pp. 529–535, Jan. 2017.
- [24] K. Niskanen, A. D. Touboul, R. C. Germanicus, A. Michez, A. Javanainen, F. Wrobel, J. Boch, V. Pouget, and F. Saigne, "Impact of Electrical Stress and Neutron Irradiation on Reliability of Silicon Carbide Power MOSFET," *IEEE Trans. Nucl. Sci.*, vol. 67, no. 7, pp. 1365–1373, Jul. 2020.
- [25] K. Matocha, G. Dunne, S. Soloviev, and R. Beaupre, "Time-Dependent Dielectric Breakdown of 4H-SiC MOS Capacitors and DMOSFETs," *IEEE Trans. Electron Devices*, vol. 55, no. 8, pp. 1830–1835, Aug. 2008.
- [26] M. Deki, T. Makino, K. Kojima, T. Tomita, and T. Ohshima, "Single event gate rupture in SiC MOS capacitors with different gate oxide thicknesses," *Mater. Sci. Forum*, vol. 778-780, pp. 440–443, Feb. 2014.
- [27] R. B. Abernethy, *The new Weibull handbook : Reliability & statistical analysis for predicting life, safety, survivability, risk, cost and warranty claims*, 5th ed. North Palm Beach: Robert B. Abernethy, 1996.
- [28] C. Martinella, R. G. Alia, R. Stark, A. Coronetti, C. Cazzaniga, M. Kastriotou, Y. Kadi, R. Gaillard, U. Grossner, and A. Javanainen, "Impact of Terrestrial Neutrons on the Reliability of SiC VD-MOSFET Technologies," *IEEE Trans. Nucl. Sci.*, vol. 68, no. 5, pp. 634–641, May 2021.
- [29] Y. Nissan-Cohen, J. Shappir, and D. Frohman-Bentchkowsky, "Trap generation and occupation dynamics in SiO<sub>2</sub> under charge injection stress," *J. Appl. Phys.*, vol. 60, no. 6, pp. 2024–2035, Sep. 1986.
- [30] D. Lucsányi, R. G. Alía, K. Biłko, M. Cecchetto, S. Fiore, and E. Pirovano, "G4SEE : A Geant4-Based Single Event Effect Simulation Toolkit and Its Validation Through Monoenergetic Neutron Measurements," *IEEE Trans. Nucl. Sci.*, vol. 69, no. 3, pp. 273–281, Mar. 2022.
- [31] J. F. Ziegler, M. D. Ziegler, and J. P. Biersack, "SRIM - The stopping and range of ions in matter (2010)," *Nucl. Instrum. Methods Phys. Res. Sect. B, Beam Interact. Mater. At.*, vol. 268, no. 11-12, pp. 1818–1823, Jun. 2010.